Turbulence, Heat and Mass Transfer 4
K. Hanjalić, Y. Nagano and M. Tummers (Editors)

Numerical study of heat and flow in a plate-fin heat exchanger with vortex generators

Ahmad Sohankar[1] and Lars Davidson[2]
[1]*Mechanical Engineering Department, Yazd University, Yazd, Iran*
[2]*Thermo and Fluid Dynamics, Chalmers Univ. of Tech., Gothenburg, Sweden*

ABSTRACT-To investigate the flow and heat structures in a plate-fin heat exchanger with vortex generators, unsteady three-dimensional DNS and LES simulations for resolutions up to about 1.2 million points were performed.The Prandtl and Reynolds numbers are 2000 and 0.71, respectively. An incompressible finite volume code, based on a fractional step technique with a non-staggered grid arrangement and a multigrid pressure Poisson solver, was used. From these simulations, the structures of heat and flow were studied by using instantaneous and time-averaged quantities such as iso-contours of velocity components, pressure, vortices, turbulent stresses, temperature fluctuations and Nusselt number. This study shows that the temperature fluctuations, turbulent kinetic energy and unsteadiness effects are stronger in the region where the longitudinal vortices are more active. A comparison between DNS and LES simulations for the present study shows that the predicted structures of fluid flow and temperature fields are similar for both methods.

1. Introduction

Compact heat exchangers are widely employed in engineering applications, especially in automotive industry, air-conditioning and refrigerant apparatus. The improvements in design of these heat exchangers have attracted many researchers for a long time to develop more compact and less expensive heat exchangers with high-energy performance. This need for high performance thermal systems has led researchers to use different augmentation methods of heat transfer. Different mechanisms such as creating electric or acoustic fields, surface vibration, fluid additive and use of a special surface geometry, may be used for heat transfer enhancement which can be classified in two groups: main-flow and secondary flow enhancement in active or passive way [1,2]. The methods such as electric or acoustic fields, surface vibration and mechanical devices are called active because they require external power, whereas the passive methods, which use a special surface geometry or fluid additive, do not require external power. Wavy wings, louvers and strip fins are examples of passive main-flow enhancement methods, while flow pulsation is an active main-flow method. The use of surface protuberances is a passive secondary flow method and based on developing boundary layers, creating swirl or vortices and flow destabilization or turbulence intensification [3]. In general, mixing the main flow, reducing the flow boundary layer thickness, raising the turbulent intensity, creating the rotating and secondary flow are main reasons for the rise of heat transfer. A comprehensive review of progress in passive heat transfer enhancement is found in Refs.2-4.In recent years, the vortex generators such as fins, ribs, wing, etc have been successfully used as a powerful way for enhancement of heat transfer in the development of modern heat exchangers.Vortex generators are special surfaces used to generate secondary flow or vortices by swirl and destabilize the flow. Due to the pressure difference between the forward and backside of vortex generators,the flow along the side edges separates and generates longitudinal vortices. Different types of vortex generators

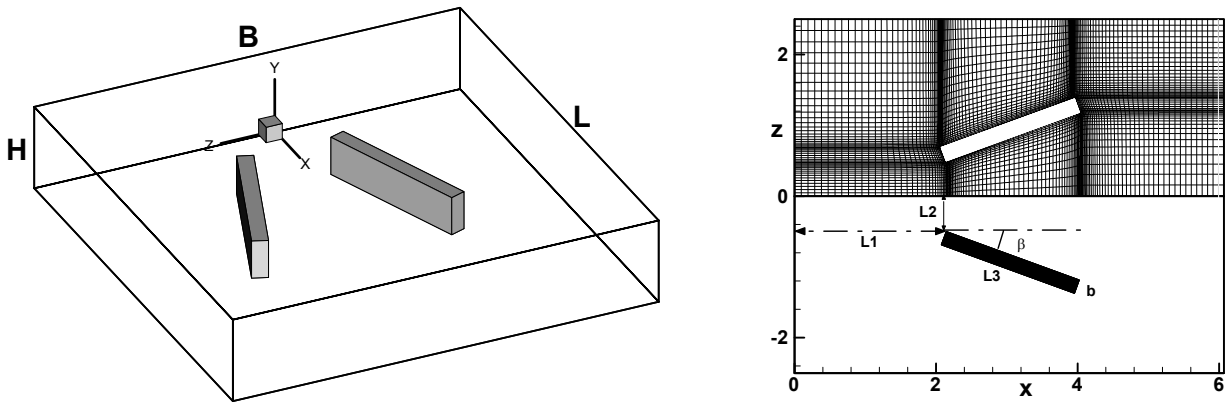

Figure 1-Left: 3D flow configuration. Right: Flow configuration and grid (DNS1, 122*98) at the channel floor, xz-plane.

such as rectangular and triangular wings and winglets,were considered for heat enhancement by Fiebig and co-workers and also other researchers, e.g. see [5-14]. The vortex generators can generate transverse, longitudinal and horseshoe vortices. These vortices have influences on the velocity and temperature fields and strongly disturb the flow structure. These factors are reasons for heat transfer enhancement by vortex generators.

In addition to heat enhancement, some other factors should be considered for choosing a type of vortex generator for real situation. First, heat transfer enhancement is usually accompanied by additional pressure or flow losses and require more power. One vital factor is manufacturability. Manufacturing of heat transfer surfaces with vortex generator should be as easy as or easier than heat transfer surfaces with other enhancement devices.

The main objective of this study is to investigate the effect of the presence of a pair of vortex generators on the heat transfer and fluid flow of a channel as a part of a plate-fin heat exchanger for Re=2000, and Pr=0.71.This study has been made to expand the previous work of the authors[10]. In this study higher Reynolds number and a finer grid are used, and also fluctuations and turbulent stresses are presented for the large eddy simulation and DNS.

2. Governing Equations, Geometry and Numerical Details

The continuity,Navier-Stokes and energy equations in dimensionless form for incompressible flow with constant fluid properties are as follows

$$\frac{\partial u_i}{\partial x_i} = 0 \tag{1}$$

$$\frac{\partial u_i}{\partial \tau} + \frac{\partial (u_i u_j)}{\partial x_j} = -\frac{\partial p}{\partial x_i} + \frac{1}{\mathrm{Re}} \frac{\partial^2 u_i}{\partial x_j \partial x_j} \tag{2}$$

$$\frac{\partial \theta}{\partial \tau} + \frac{\partial (u_i \theta)}{\partial x_i} = \frac{1}{\mathrm{Re}\,\mathrm{Pr}} \frac{\partial^2 \theta}{\partial x_i \partial x_i} \tag{3}$$

In this work, an incompressible finite volume code, based on a fractional step technique with a non-staggered grid arrangement and a multigrid pressure, was used. The scheme was implicit in time, and a second order Crank-Nicolson scheme was used. All terms were discretized using the second-order central differencing scheme. In the large eddy simulations (LES) a one-equation dynamic subgrid model [15,16] was used to predict the SGS turbulence. The details of the numerical solution procedure for the DNS and LES simulations and also subgrid models are found in Refs. 10 and 15-17.

The physical problem considered in this study is a three-dimensional channel flow as part of a plate fine compact heat exchanger, see Fig. 1. Two three-dimensional inclined blocks are mounted on the floor of the horizontal channel as vortex generators to enhance heat transfer. The flow is described in a coordinate system (*x, y, z*) in which the *x*-axis is aligned with the inflow, streamwise direction, the *z*-axis is in the spanwise direction and the y-axis is perpendicular to both *x* and *z*, see Fig.1.The two vortex generators are mounted with an angle of incidence,β, to the streamwise direction, *x*-axis. The sides of the vortex generators in the *x*-*z*-plane are denoted with *L3* and *b,* and the height of the vortex generators in the *y* direction is *h*. The sides of the channel are denoted with *L, H* and *B* in *x, y, z* directions, respectively.

An incompressible flow with constant fluid properties is assumed. The Reynolds number is defined as $\mathrm{Re} = UH/\upsilon$, where U is a constant inflow velocity. All geometrical lengths are scaled with *H*, the height of the channel. Velocities are scaled with U, and physical times with H/U. In this work, (*H, L, B)* are set to (1,6,5) and *(L1, L2, L3, b, h*, β) are set to 2, 0.5, 2, 0.2, 0.5 and 10^{o}-30^{o}, respectively. The dimensionless temperature is defined as $\theta = (T - To)/(Tw - To)$, where Tw is the constant temperature at the channel walls and the vortex generators and To is the constant inflow temperature. The pressure is scaled with ρU^2, where ρ is the flow density.

The time-marching calculations were started with the fluid at rest, and a constant dimensionless time step, Δt=0.01, was used. The grid distribution was non-uniform body-fitted in the *x*-*z*-planes. The distance from the vortex generators surface to the nearest grid point was set about 0.01 for all calculations in this study. The hyperbolic tangent function was used for stretching, see Fig. 1. A uniform grid between the nodes was used in the *y* direction. In the present study, a resolution of *122*34*98* grid points in the (*x, y, z*) directions is used for LES and DNS (denoted as *DNS1*) simulations, see Fig. 1. A finer resolution of *162*50*146* grid point is also employed for DNS simulations and denoted as *DNS2*. The following boundary conditions were used. A uniform flow (U=1, v=w=θ=0) was prescribed at the inlet. At the outlet, the convective boundary condition $(\frac{\partial u}{\partial \tau} + U\frac{\partial u}{\partial x} = 0)$ was used for streamwise velocity component. Neumann condition was used for v, w and θ at the outlet. No-slip conditions were prescribed at the vortex generators surfaces and the lower (*y*=0) and upper (*y*=*H*) wall of the channel. θ is set to one on the vortex generators and the channel walls where $T = Tw$. Symmetry conditions $(\frac{\partial u}{\partial z} = \frac{\partial v}{\partial z} = \frac{\partial \theta}{\partial z} = w = 0)$ were used in the spanwise direction. The normal derivative for the pressure was set to zero at all boundaries.

3. Results and Discussion

To investigate the flow and heat structures in a plate-fin heat exchanger with vortex generators, unsteady three-dimensional simulations were carried out. The structures of the velocity and temperature fields are clearly observed in figure 2, where the time averaged

velocity components, streamwise vortices, pressure and normalized temperature contours are shown. Based on the results of this study, it is observed that when the vortex generators are exposed to the main flow, due to pressure difference between two sides of vortex generator, flow separation occurs and longitudinal vortices are generated. These vortices detach from the vortex generators and form counter-rotating vortex pairs downstream of the vortex generators, e.g. see plot for streamwise vortices, *Wx*. One of the vortices rotates in clockwise and the other in the counter-clockwise direction. These vortices make a down-wash movement toward the centre part of channel between the two vortex generators and also an up-wash movement away from the hot lower wall in the region outside of the vortex generators. These down-wash and up-wash flows increase mixing of cold fluid in the middle of the channel and hot fluid adjacent to the channel walls, which enhances heat transfer (see Fig. 2). The shape and the distance between the cores of the longitudinal vortices change as these vortices move downstream of the vortex generators. It is also observed that the cross section of the vortices change from a circular shape close to the vortex generators to an elliptic shape far from the vortex generators (see Fig. 2). The spaces between the cores in the spanwise direction are 2.2 and 2.5 at x=4.5 and x=6, respectively. Also the strength of the vortices changes as these vortices develop downstream. For example, the magnitude of the streamwise vortices at the centre of each vortex are 10.7 and 9.7 at x=4.5 and x=6, respectively. A significant change in streamwise velocity deficit in the core of the vortices was observed. As the vortices move downstream, the streamwise velocity in their centre part increases (or velocity deficit decreases) from 0.35 at x=4.5 to 0.57 at x=6.

There are strong interactions between the longitudinal vortices and the boundary layer on the walls of the channel, especially the lower wall. These interactions affect the structure of the velocity or the thermal boundary layer by thinning it in the downwash region and thickening it in the up-wash region on the lower wall while the opposite trend occurs on the upper wall, see streamwise velocity and normalized temperature contours in Fig. 2.

As is seen from the pressure and the streamwise vortices plots in Fig. 2, the centre of the vortices correspond to the position of minimum pressure and maximum vortex strength. For example, at x=6, the centre positions are located at y=0.39 and z=±1.24 with Wx=9.64, see Fig. 2.

Figure 3 shows the time-averaged turbulent kinetic energy and the temperature fluctuations. From Figs. 2 and 3, it is clear that the levels of the kinetic energy and the temperature fluctuations are high in the regions where the secondary flow or vortices are more active. This means that turbulence is generated by the longitudinal vortices. As is seen from Fig. 3, the turbulent kinetic energy is high in the vortex cores and also near the lower wall. Due to diffusion of turbulent kinetic energy, it becomes weaker far from the bottom wall and close to the upper wall. By comparing the normalized temperature contours (Fig. 2) and the temperature fluctuations (Fig. 3), it is observed that the locations of high temperature levels approximately correspond to those of high temperature fluctuations. The temperature fluctuations are strong close to the walls especially near the bottom wall and in the upwash region, see Fig. 3.

As mentioned above, the plots in Figs. 2 and 3 are time-averaged quantities and it is important to note that the structures of the flow and temperature field vary with time. This is clearly observed from time evolution of normalized temperature and velocity components at a chosen point downstream of one of the vortex generators, where the longitudinal vortex is active, see Fig. 4. This figure indicates that the flow and the temperature vary with time in this region. This unsteady behaviour is also observed in different regions of the calculation domain but with different levels of unsteadiness. The level of fluctuations (or unsteadiness) for temperature, pressure and velocity components are higher in the downstream region than in the upstream region.

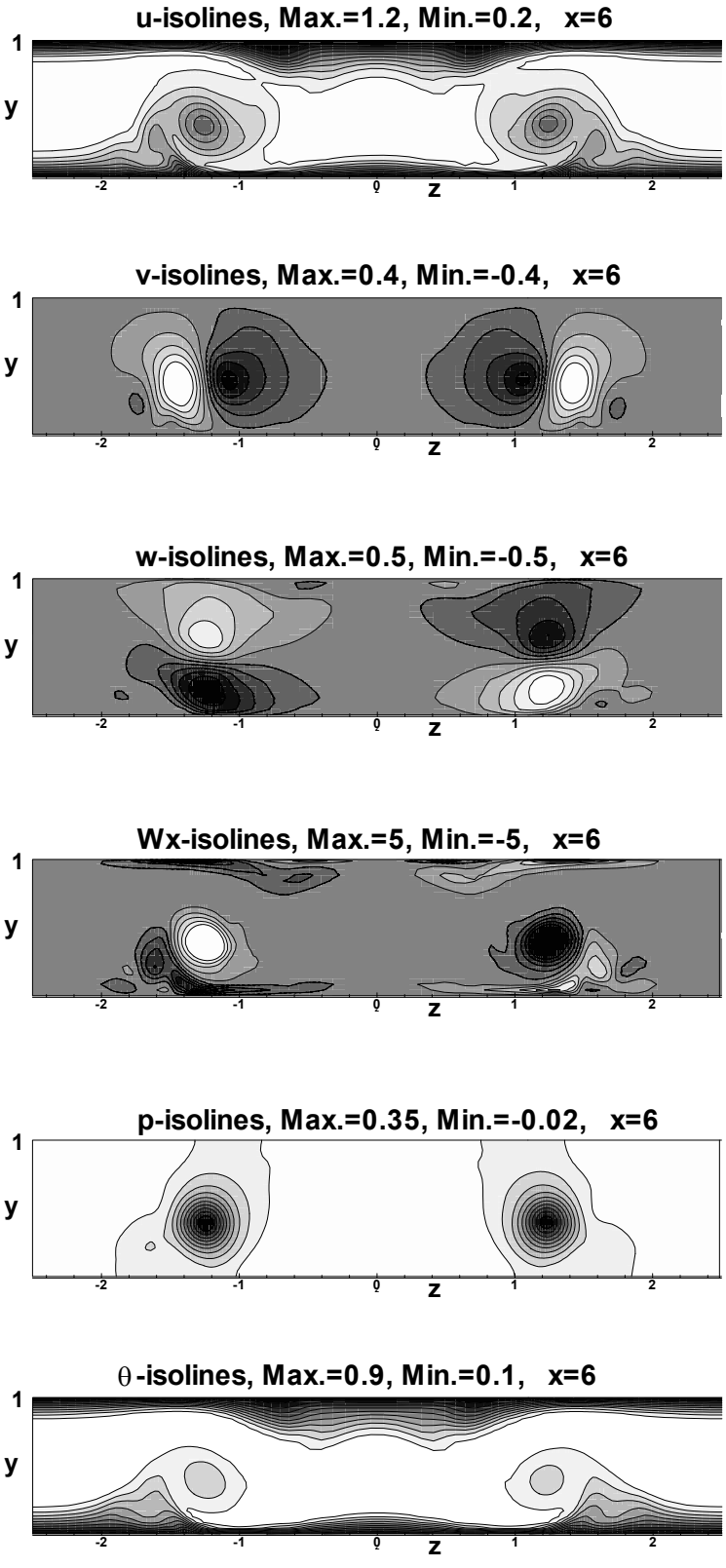

Figure 2:From top to bottom: time averaged velocity components (u, v, w), streamwise vortices, pressure and normalized temperature isolines in one section downstream of vortex generators. DNS2, x=6, β=20.

By considering time evolution of flow and temperature at different points in the calculation domain, it is found that the unsteadiness is more dominant around the vortex generators, wake and separation regions, and in the downstream of the vortex generators. Not much unsteadiness is found upstream of the vortex generators. Previous work of the authors[10] it was shown that the flow and temperature were steady for Reynolds number up to 1000. The unsteady behaviour is also observed from Fig. 4 where the contours of the instantaneous local Nusselt numbers on the lower wall and vortex generators at one time instant are illustrated. By comparing this figure with the time-averaged local Nusselt number, (time-averaged one is not shown here), it is observed that the level of unsteadiness is large around and downstream of the vortex generators, where the vortices are active. By considering Fig. 4, it is seen that there are some differences in the structure of the temperature field behind the two vortex generators due to the unsteadiness, while the geometry is symmetric. By referring again to Fig. 4, it is possible to draw other results. As is seen from Fig. 4, a system of vortices generates and bends around vortex generators in horseshoe pattern with high local Nusselt number. The local Nusselt is also high at the upper side of the vortex generators, especially at the leading edge and the outer edge. Furthermore, there is an enhanced heat transfer (or high local Nusselt number) downstream of the vortex generators, where the longitudinal vortices mix the cold and hot fluids. It is important to mention that we have not found any experimental or numerical investigation to compare with this study except reference 10 which provided results for lower Reynolds numbers. Of course, there are some investigations similar to this study but with different geometries of the vortex generators, e.g. see references12-14.

The variation of time- and spanwise-averaged Nusselt numbers, Nu(x), in the streamwise direction for different angles of incidence, resolutions and simulations (LES and DNS) are shown in Fig. 5. By increasing the angle of incidence from 10^o to 30^o, the NU(x) increases in the regions where the vortex generators are present and also downstream of them. On the other hand, the variations of Nu(x) are approximately similar in the upstream of vortex generators. There is a peak on each of the curves of Nu(x) in front of the vortex generators, where the horseshow vortices form. After this peak and along the vortex generators, the level of Nu(x) gradually decreases and reaches to an approximately constant level for all cases except for β=30. Along the vortex generators for case β=30, Nu(x) decreases and then increases to a new peak at the trailing edge of the vortex generator.

A comparison between the DNS and LES simulations for the present study shows that the predicted structures of flow and temperature field are similar for both methods. As is seen from Fig. 5, the variations of the Nu(x) for these cases are approximately similar. The agreement between case DNS2(finer grid) and LES is good especially along and downstream of the vortex generator, while there is a difference between the results for case DNS1 and DNS2 downstream of the vortex generator. Thus, it is possible to obtain similar results by using a LES simulation with relatively fine grid instead of a DNS with very fine grid.

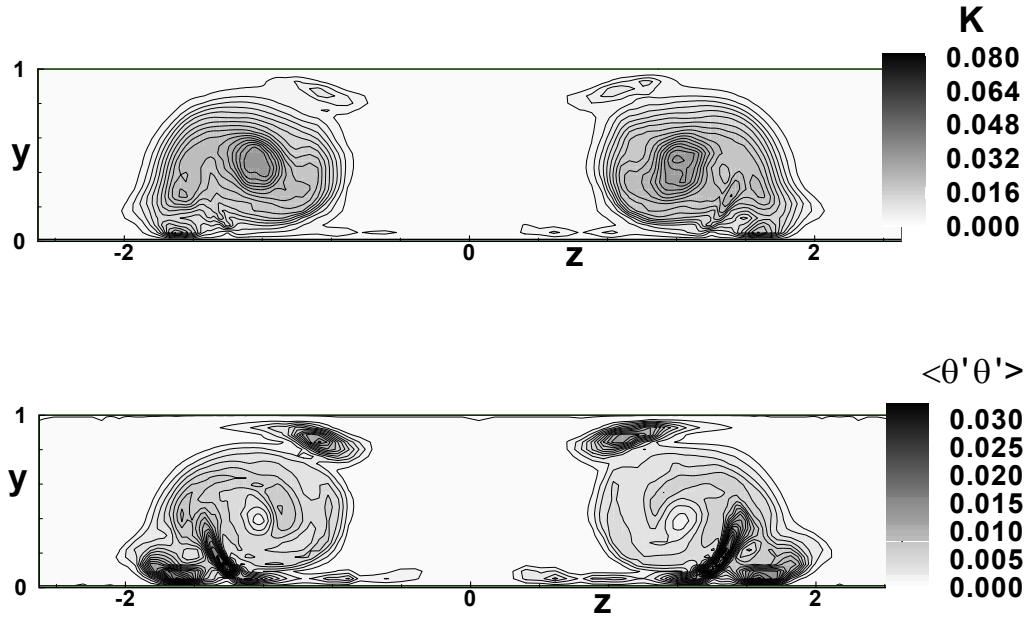

Figure 3: Time-averaged temperature fluctuations (top) and turbulent kinetic energy (bottom) isolines, DNS2, β=20.

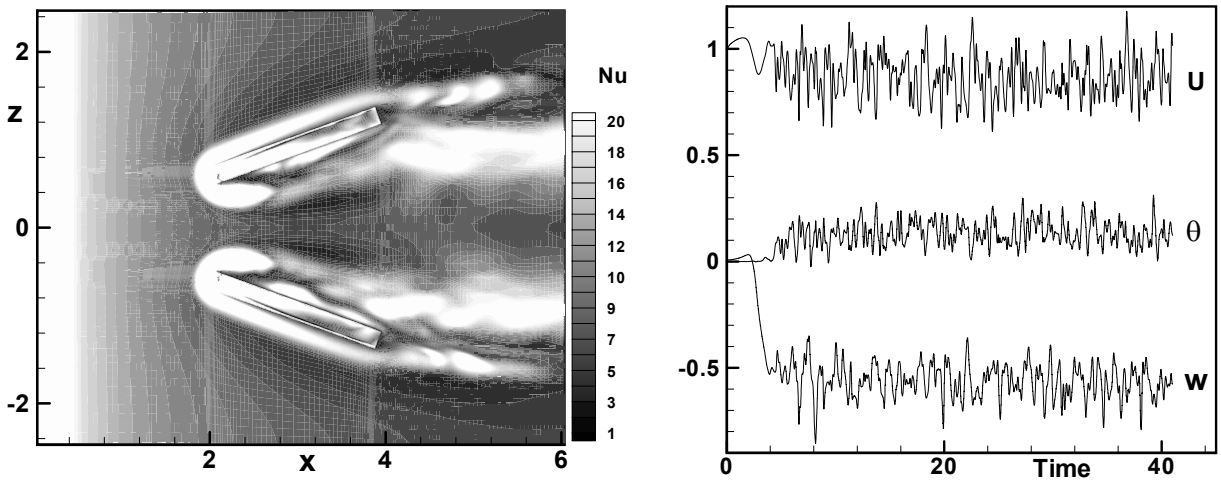

Figure 4-Left: Instantaneous local Nusselt number contours, Nu (x, z), at one time instant on the channel floor and vortex generators surfaces. Right: Time evolution of normalized temperature and velocity components at a chosen point (x=6, y=0.24, z=-1.2, see Fig. 1), DNS2, β=20.

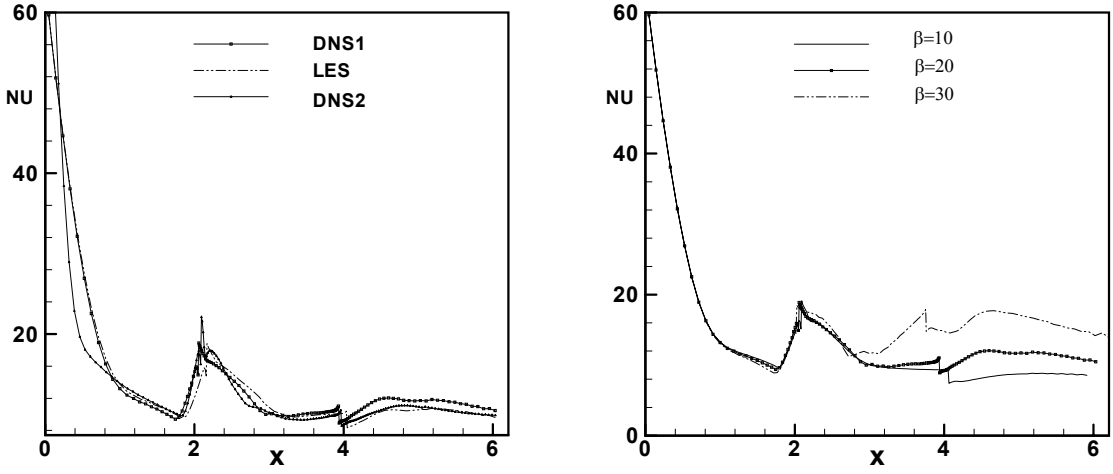

Figure 5: Time- and spanwise-averaged Nusselt number vs. x , Nu(x). Right: different angle of incidence, DNS1; Left: different resolutions (DNS1, DNS2) and methods (LES, DNS), β=20.

References

1. R.L.Webb, Principles of Enhanced Heat Transfer, John Wiley & Sons, Chichester, UK, 1994.
2. A. M. Jacobi and R.K. Shah, Heat transfer surface enhancement through the use of longitudinal vortices: A review of recent progress, Experimental Thermal and Fluid Science, 11:295-309, 1995.
3. M. Fiebig, Vortices, generators and heat transfer, Trans ICHemE., 76 Part A:108--123, 1998.
4. A. M. Jacobi and R.K. Shah, Air-side flow and Heat transfer in compact heat exchangers: A discussion of enhancement mechanisms, heat transfer engineering, 19:29-41, 1998.
5. M. Fiebg, Embedded vortices in internal flow: heat transfer and pressure loss enhancement, J. Heat and Fluid flow, 16:376-388,1995.
6. Fiebig, A. Valencia, and N. K. Mitra, Wing-type vortex generators for fin-and-tube heat exchangers, Experimental Thermal and Fluid Science, 7:287--295, 1993.
7. G. Biswas, N. K. Mitra, and M. Fiebig, Heat transfer enhancement in fin-tube heat exchangers by winglet type vortex generators, International Journal of Heat and Mass Transfer, 28:283-291, 1994.
8. M. C. Gentry and A. M. Jacobi, Heat Transfer Enhancement by Delta-Wing Vortex Generators on a Flat Plate: Vortex Interactions with the Boundary Layer, Exp. Thermal Fluid Sci., 14:231-242, 1999.
9. B. D. Storey and A. M. Jacobi, The Effect of Stream wise Vortices on the Frost Growth Rate in Developing Laminar Channel Flows, International Journal of Heat and Mass Transfer, 42:3787-3802, 1999.
10. A. Sohankar and L. Davidson, Effect of inclined vortex generators on heat transfer enhancement in a three- dimensional channel, Numerical Heat Transfer: Applications, 39:2001.
11. V. Zimparov, Enhancement of heat transfer by a combination of a single-start spirally corrugated tube with a twisted tape, Experimental Thermal and Fluid Science, 25:535-546, 2002.
12. K. Torii, K. M. Kwak, K. Nishino, Heat transfer enhancement accompanying pressure-loss reduction with winglet-type vortex generators for fin-tube heat exchangers, I. J. of Heat and Mass transfer, 45:3795-3801, 2002.
13. E. Kim, J.S. Yang, An experimental study of heat transfer characteristics of a pair of longitudinal vortices using color capturing technique, I. J. of Heat and Mass transfer, 45:3349-3356, 2002.
14. J. S. Yang, J. K. Seo, K. B. Lee, A numerical analysis on flow field and heat transfer by vortices using color capturing technique, I. J. of Heat and Mass transfer, 45:3349-3356, 2002.
15. A. Sohankar, L. Davidson and C. Norbeg, Large eddy simulation of flow past a square cylinder: comparison of different subgrid scale models, ASME, J. Fluids Eng., 122:39-47,2000. See also Erratum J. Fluids Eng., Vol. 122 pp.643.
16. L. Davidson Large eddy simulation: a dynamic one-equation subgrid model for three-dimensional re-circulating flow. In 11th Int. Symp. on Turbulent shear Flow, Grenoble, volume 3, page 26.1-26.6, 1997.
17. A. Sohankar, Numerical Study of Laminar, Transitional and Turbulent Flow Past Rectangular Cylinders, PhD. thesis, Dept. of Thermo and Fluid Dynamics, Chalmers University of Technology, Gothenburg, 1998.